ADVANCED SENSOR RESEARCH Open Access
www.advsensorres.com

Controlled Molecular Diffusion in Fluorescent Polymer Films for Label-Free Detection of Volatile Organic Compounds

Heba Megahd, Marco Carlotti, Martina Martusciello, Laura Magnasco, Andrea Pucci, Davide Comoretto, and Paola Lova**

Aggregation-induced emission has eliminated the problem of fluorescence quenching in the solid state, making molecules with this property excellent candidates for vapor sensing due to their portability and ease of interpretation. Here, films of polystyrene / 2-[4-vinyl(1,10-biphenyl)-40-yl]-cyanovinyljulolidine copolymers are reported that exhibit aggregation-induced emission behavior for the detection of toluene, *m*-xylene, dichloromethane, and chloroform. After exposure to the analytes, the emission of the copolymers shows significant changes in intensity and spectral shape corresponding to the reduced microviscosity of the molecular environment. However, these changes are similar for different analytes, resulting in low chemical selectivity. Therefore, label-free selectivity is achieved by controlling the molecular diffusion of the four vapor analytes within the films using the Flory–Huggins solution theory with capping layers of cellulose acetate (CA) and poly(vinyl alcohol) (PVA) polymers.

1. Introduction

Human exposure to volatile organic compounds is a known cause of health complications,[1] making their detection essential in industrial or urban settings.[2] Unfortunately, the current widely employed quantitative analysis is cumbersome, complicated, and cannot be done by untrained personnel.[3] As such, simple and fast sensors are needed for environmental and industrial monitoring. In this context, fluorescent indicators have long been a reliable means of chemical sensing,[4] specifically widely used in biology and tissue imaging.[5] However, their utility is often limited to solution because of fluorescence quenching in the solid state.[6] The phenomenon of aggregation-induced quenching has been extensively studied and is commonly attributed to increased non-radiative relaxation pathways for the fluorophores as the distance between them decreases, and intermolecular forces start modifying the electronic states.[7] In this context, the discovery of fluorophores exhibiting an enhanced quantum yield in the solid state or aggregates[8] has presented a paradigm shift for applications including light-emitting devices,[9] smart responsive materials,[10] and sensing.[11] These fluorophores exhibit an aggregation-induced emission (AIE) where the luminogens are referred to as AIEgens, as a direct opposite to the aforementioned aggregation-induced quenching phenomenon.[12] Multiple mechanisms of fluorescence enhancement exist for AIEgens, including J-aggregate formation, twisted intramolecular charge transfer, excited-state intramolecular proton transfer, and restriction of intramolecular motion.[11] For the latter, the immobilization of the AIEgens in the solid state or aggregates blocks the non-radiative vibrational and rotational relaxation pathways. Fluorescent molecular rotors (FMRs) are a common example of AIEgens used as viscosity probes.[13] This typology of AIEgens are molecules with chromophore units linked with flexible bonds that are free to rotate in solution (segmental mobility) and whose rotation is restricted in aggregates, in the solid state and even in viscous media, causing radiative relaxation and high fluorescence quantum yield, as schematized in **Figure 1**a. Thin films of polymers employing AIE have seen increasing interest as vapor sensors.[14] In fact, the integration of such AIEgens in polymers has been demonstrated as a viable way to make fluorescent thin films sensitive to vapor analytes, where the change in the microviscosity due to the solvent-induced plasticization of the polymer modulates the fluorescence intensity.[15] Equation (1) describes the relationship between the fluorescence quantum yield (ϕ) and the viscosity (η), where c is an experimental constant, and γ is the viscosity sensitivity of the FMR[16] in typical Förster–Hoffmann behavior.[17] The viscosity sensitivity of FMRs depends strongly on their molecular design and has the highest theoretical value of 0.66.[18] Since quantum yield variations are perceived as intensity variations, this provides

H. Megahd, M. Martusciello, L. Magnasco, D. Comoretto, P. Lova
Department of Chemistry and Industrial Chemistry
University of Genoa
via Dodecaneso 31, Genoa 16146, Italy
E-mail: davide.comoretto@unige.it; paola.lova@unige.it
M. Carlotti, A. Pucci
Department of Chemistry and Industrial Chemistry
University of Pisa
Via Giuseppe Moruzzi 13, Pisa 56124, Italy
The ORCID identification number(s) for the author(s) of this article can be found under https://doi.org/10.1002/adsr.202300114

DOI: 10.1002/adsr.202300114

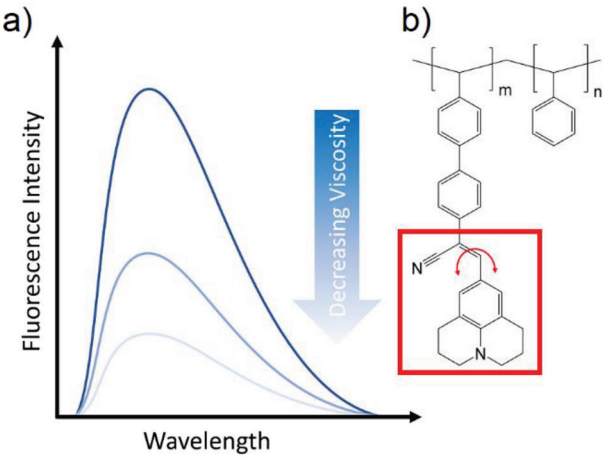

Figure 1. a) Fluorescence quenching of AIEgens in an environment of decreasing viscosity, b) structure of P(STY-*co*-JCBF) CP.

a straightforward transduction signal where the fluorescence intensity is expected to increase with increasing viscosity.

$$\log \phi = c + \gamma \log \eta \tag{1}$$

Previously, a copolymer of polystyrene (STY) and the AIEgen 2-[4-vinyl(1,1*0*-biphenyl)−4*0*-yl]-cyanovinyljulolidine (JCBF) showed fast quenching with different kinetics upon exposure to different volatile organic compounds.[19] JCBF should indeed act as a viscosity-sensitive AIEgen in the glassy polystyrene (PS) matrix, owing to the presence of the cyanovinyljulolidine moiety (red square, Figure 1b) and the rotation around the julolidine–vinyl bond, as shown in the chemical structure of the copolymer P(STY-*co*-JCBF) in Figure 1b, henceforth referred to simply as copolymer (CP). The copolymerization was proven to lead to faster quenching as compared to only dispersing JCBF in a PS matrix.[19] However, without chemical labeling, some analytes cause a similar response, which is a common limitation of dye-based systems.[20] This is especially relevant as the principal mechanism of sensing for the AIEgen in question is not a chemical reaction but rather the physical resistance to molecular rotation caused by the viscosity of the effective medium.

Multiple approaches have been implemented to increase the selectivity of optical readout sensors circumventing chemical labeling, including utilizing arrays of responsive films and using multivariate analysis to identify the analytes.[21] Another is adding a capping layer that selectively influences the diffusion of possible vapors to the active medium. This approach has been demonstrated as a means of selectivity in sensors based on semiconducting polymers[22] as well as colorimetric solvent sensors.[20] Importantly, for sensors based on thin polymer films, the interactions between the polymer and the analyte have been shown to rule the diffusion and hence the kinetics of the response. We have indeed previously shown that engineered multilayered polymer structures significantly influence the diffusion behavior in photonic sensors based on the Flory–Huggins solution theory.[23]

The specific polymer–solvent interactions, represented by the Flory–Huggins interaction parameter χ, of a polymer–solvent

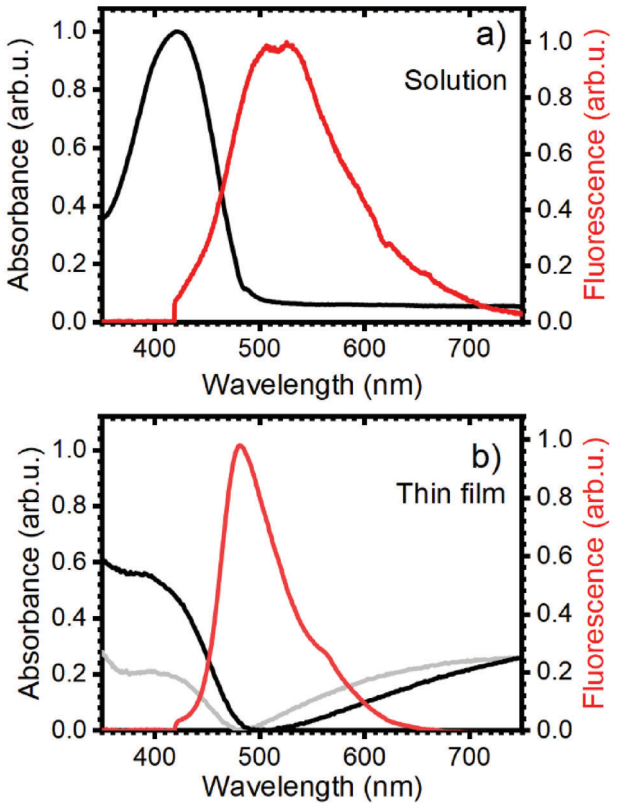

Figure 2. Normalized absorbance (black) and fluorescence (red) of P(STY-co-JCBF) a) in chloroform solution and b) in thin film collected at normal incidence (black) and by tilting the sample by ≈20° (light grey) on a fused-silica substrate.

pair are also expected to influence the quenching kinetics. As the value of χ increases, the permeability of the solvent in the polymer strongly decreases,[24] causing a barrier effect.[25]

The parameter can be calculated as in Equation (2) using the molar volume of the analytes (V_M) and the squared difference between the Hildebrand solubility parameters for the components considered ($\Delta\delta^2$) (neglecting entropic contributions).[26] The latter represents the difference in the density of cohesive energy between polymers and solvents such that higher solubility is represented by a smaller $\Delta\delta^2$.

$$\chi = V_{\mathrm{M}} \frac{\Delta\delta^2}{RT} \tag{2}$$

In this work, we report on the fluorescence of thin CP films incorporating AIEgens as well as using polymer barrier layers to control the selectivity of disposable AIE-based vapor sensors for toluene, chloroform, dichloromethane, and *m*-xylene.

2. Results and Discussion

2.1. Copolymer Absorbance and Fluorescence

Figure 2 compares the absorbance (black) and fluorescence (red) of the CP in solution (a) and as a thin film (b). The absorbance in chloroform solution in Figure 2a shows a high absorbance in the

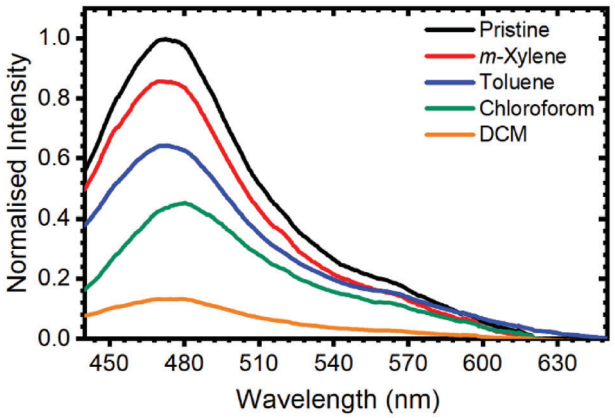

Figure 3. Fluorescence quenching: spectra collected for the unexposed film (black) and after exposure to vapors of chloroform, *m*-xylene, toluene, and DCM for one minute.

violet and UV with a peak at ≈420 nm. The thin film (black line in Figure 2b) shows a complex spectrum with intense absorption in the UV and violet range followed by a broad signal in the visible range. This second signal is associated with the presence of an interference pattern. The nature of this signal is confirmed by comparing the spectra of the film collected at a normal incidence (black line) and by tilting the sample by ≈20° (light gray line). While the spectral shape on the signal in the UV and violet range remains mainly unchanged tilting the sample, the peak positioned in the long wavelength side of the spectrum shifts with the angle, which is a characteristic behavior of the interference pattern.

The photoluminescence of the solution peaks at about 520 nm and extends almost through the entire visible spectrum. Conversely, the film emission is blue-shifted, narrower, and peaked at 480 nm. The effect of different starting concentrations on the fluorescence of the cast films and the impact of their drying is reported in Figure S2 (Supporting Information). Drying the residual solvent in the film causes an increase in the fluorescence intensity due to the rise in the viscosity of the film.

2.2. Fluorescence Quenching

The same principle applies when exposing thin films of the CP to different analytes. **Figure 3** shows the fluorescence spectrum of the CP thin film cast on glass before exposure to any analytes (black line) and after one minute of exposure to vapors of *m*-xylene (red), toluene (blue), chloroform (green), and dichloromethane (DCM, orange). All the spectra are normalized to their initial intensity for a clear comparison. The spectra show that after one minute of exposure to the vapors, the fluorescence is already noticeably quenched for all the analytes, with quenching extent highest for exposure to DCM followed by chloroform, toluene, and finally *m*-xylene. Also, minor spectral shifts of the emission peak are observed for all analytes. From Equation (1), the intensity is expected to decrease with decreasing viscosity and thus with increasing concentration of vapor in the polymer film. As the vapor pressure of a liquid (P_v) is correlated to its concentration, we examine the relationship between P_v (see **Table 1**) and the

Table 1. Vapor pressure for all tested analytes and Flory–Huggins interaction parameters for the used analyte-polymer pairs.

Solvent	Pv [kPa][27]	$T_{0.2}$ [min]	χ_{PS}	χ_{PVA}	χ_{CA}
m-xylene	1.1	8.8	1.14	3.71	4.64
Toluene	3.9	2.9	0.82	2.88	3.65
Chloroform	25.5	2.2	0.41	1.78	2.31
DCM	57.8	0.9	0.14	0.98	1.33

fluorescence quenching extent after one minute for our system. Indeed, the strongest quenching takes place on exposure to DCM (P_v = 57.8 kPa), followed by chloroform (P_v = 25 kPa), toluene (P_v = 3.9 kPa) and the slowest being *m*-xylene (P_v = 1.1 kPa). The different quenching efficiency appears affected by to the different analyte vapor pressure. The quenching time related to the vapor pressure is reported in Figure S3 (Supporting Information). There, we report the time needed for the CP to reach 20% of its original intensity ($T_{0.2}$) for the different analytes (see also Table 1). $T_{0.2}$ appears clearly correlated to the inverse of the vapor pressure. This suggests that the analyte concentration in the environment mainly dominates the quenching extent.

2.3. Polymer–Vapor Interactions

As stated in the introduction, the Flory–Huggins interaction parameter, χ, of a polymer–solvent pair is also expected to influence the quenching kinetics in polymer matrices. This is used as a differentiation mechanism to increase the selectivity of the sensor using capping layers with different solubility in the analyte than the PS comprising most of the matrix of the CP. The values of the Hildebrand solubility parameters for both polymers and analytes, as well as the molar volume of the latter, have been retrieved from literature[26] and used to calculate χ for all the analyte-polymer pairs investigated. Table 1 reports the Flory–Huggins interaction parameter that exists between all the analytes and PS, which is used as an approximate equivalent for the CP (due to the high mole percent of PS in the CP), and for two other polymers: PVA and CA used in the study. These polymers were also selected as their solvents do not interact strongly with the CP, allowing sequential spin-coating of capping layers without damaging the fluorescent film (see materials and methods section).

The CP fluorescence quenching observed in Figure 3 appears to be also correlated to χ as it is stronger for solvents displaying lower χ with PS, as expected. This suggests the interaction with DCM is the strongest and hence is estimated to be the fastest, and the trend continues for the other analytes, with the slowest being *m*-xylene.

On the other hand, lower and more diverse solubilities were retrieved for the three molecules with respect to PVA and CA (higher χ).[26] As such, the two polymers are anticipated to slow the diffusion speed of the non-polar toluene and *m*-xylene, also having larger molecular sizes than chloroform and dichloromethane.[26] Therefore, simply employing one or both of these materials as capping layers can, in principle, rule the diffusion kinetics of the analytes to the sensitive CP film, thus making the response to the different analytes more distinguishable, achieving higher selectivity. Layers of the CP of ≈0.5 µm

thickness were thus capped with PVA and CA films of roughly 0.5 and 1 μm, respectively (see thickness profiles in Figure S4, Supporting Information). Three sets of samples were made, one of CP covered by a single layer of CA, one of CP covered by a layer of PVA and another of CP covered by CA, then PVA in such order.

2.4. Quenching Dynamics

To get a more comprehensive view of the quenching during exposure, **Figure 4** shows the intensity of fluorescence at the peak emission wavelength of the tested films as a function of the exposure time (contour plots showing the whole exposure for all wavelengths are reported in Figures S5–S8, Supporting Information). While the CP films are surely sensitive to all the analytes, it is rather complex to distinguish them from the other by analyzing only emission intensity quenching. At the beginning of the exposure for the CP film (Figure 4a), the quenching rate is observably different for all analytes, as seen from the slope of the lines. After the relatively fast initial quenching stage, the quenching slows down to ultimately reach an equilibrium. Indeed, after reaching equilibrium, the quenching extent values are rather similar for all the analytes (Figure 4a, summarized below in Figure 4e), thus making the system hardly suitable for specific detection. Capping the CP with CA, modifies the quenching dynamics, which results slowed down for the analytes with the largest molar volume, which are toluene and *m*-xylene (Figure 4b). However, the system reaches the equilibrium in a rather fast timeframe, making again the analytes difficult to distinguish. Conversely, PVA capping instead provides better diffusion kinetic, and therefore fluorescence quenching is significantly slower than in the previous cases. This facilitates the recognition. However, non-unique intensity values marked with "*" in Figure 4c) induce uncertainty in the measurement. Last, employing CA and PVA as capping layers slows the kinetics and modifies the equilibrium state, which is now different for chloroform and DCM, thus allowing full selectivity among the four analytes (Figure 4d).

For the CP film, different analytes lead to very similar long-term quenching to less than 10% of the initial signal (Figure 4e), which means it is difficult to distinguish the different analytes through intensity observation alone. However, the introduction of the capping layers changes the perspective. For example, using the CA capping layer, the quenching of the *m*-xylene is delayed, which establishes a mechanism to differentiate between the aromatic hydrocarbons *m*-xylene and toluene. The polar PVA layer on its own decreases the quenching extent for all analytes significantly (ranging from ≈20% for DCM to 80% for toluene), but more so for the non-polar *m*-xylene and toluene. However, the induced difference in quenching intensity for the chlorinated solvents (around 30%) also allows for their differentiation. Finally, using two capping layers of different materials provides a distinct intensity difference between the chlorinated and aromatic compounds, making using multiple barrier layers a viable possibility for future developments in selective sensors.

Further examination of the quenching dynamics reveals more information about the diffusion of the analytes in the films. First, it is notable that there are different regimes during the exposure for several film-analyte pairs. For example, the exposure of the

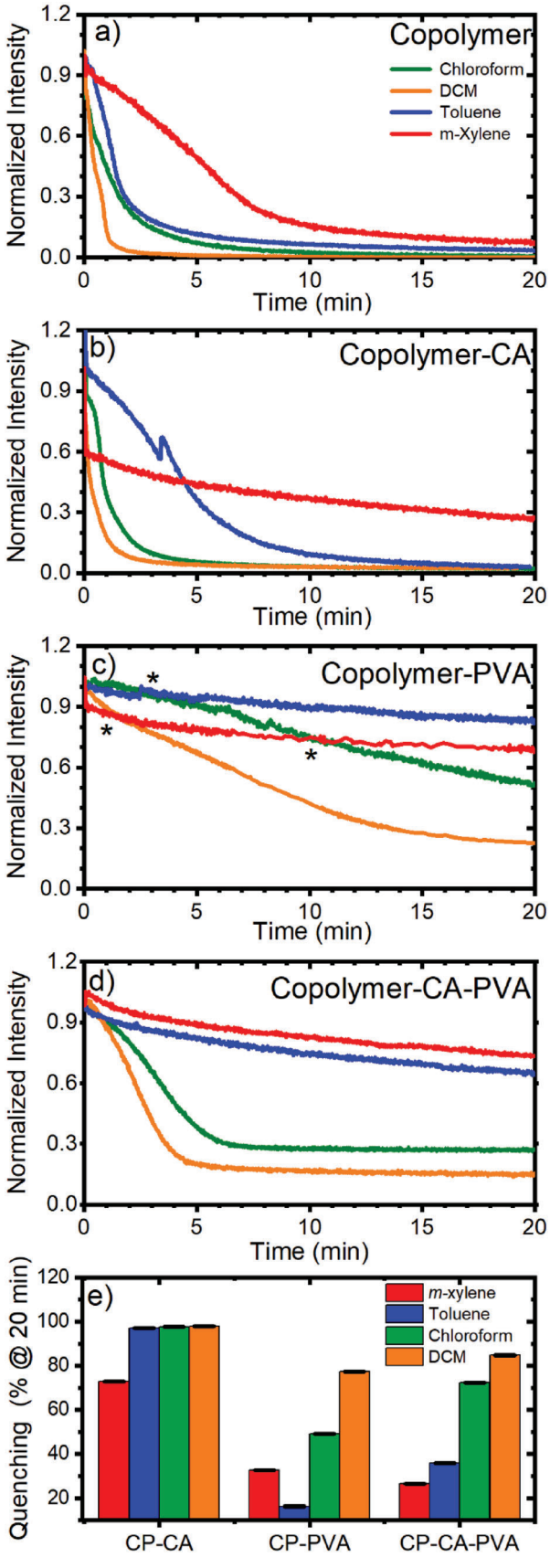

CP film to DCM and chloroform, both chlorinated compounds, causes a fast quenching in the first minute, followed by a slightly slower regime which quickly flattens out (Figure 4a). In the case of the exposure of the CP film to toluene, the quenching instead is at first slow, then speeds up after around 36 s and then slows down again for exposure longer than 100 s. Unexpectedly, the addition of a CA film on top of the CP (Figure 4b) causes an initial increase in the quenching rate on exposure to *m*-xylene with respect to the pristine copolymer. Then, in a clear 2-step mechanism (see Figure S9b, Supporting Information), the quenching slows down to a steady rate. For both toluene and chloroform, the quenching rates instead decrease, and a sharp increase in intensity occurs after around 4 s for both, returns to normal, and then occurs again at around 200. As for the DCM, no significant change is noted. Conversely, as shown in Figure 4c, the CP film capped with PVA displays a substantial variation in the quenching kinetics, slowing down for all analytes diffusion and becoming linear. This might be due to the polar nature of PVA films. However, the influence on the rate of quenching is different for each analyte. Finally, for films composed of three layers, besides slowing the diffusion and quenching, the intensity reached a plateau for the chlorinated analytes chloroform and DCM (Figure 4d). On the other hand, the quenching caused by exposure to toluene and *m*-xylene is much slower, and linear in the observed time frame, allowing their easy optical recognition from the chlorinated compounds. Clearly, it is evident that for the same analyte, the fluorescence quenching kinetics and extent are influenced strongly by the capping layers. The sudden changes in the intensity in the initial part of the exposure for CP on its own and that capped with CA might be attributed to the occurrence of Langmuir adsorption first as a fast mechanism.[28] The following linear portion of the quenching is then assumed to be controlled by the diffusion related to the Flory–Huggins parameter.

The quenching rate (i.e., $(\Delta I/I_0)/\Delta t$)) was extracted by fitting the initial linear part of the fluorescence quenching of Figure 4, not considering the rapid initial drops occurring for example in CP-CA films on exposure to *m*-xylene (Figure 4b, red line). In this time domain, the diffusion is considered fickian as accumulation is negligible.[29] The extracted rate is reported in **Figure 5** for all the different film-analyte systems (black squares, right axis). It is worth noting that the different values for the rate imply very different quenching kinetics for the systems, with the slowest being the PVA-capped one.

In addition, the effective Flory–Huggins parameter χ_{eff} (which is the thickness-averaged χ for the polymers forming the multilayered films) was calculated and multiplied by P_v and the value is reported in red in Figure 5. There seems to be a general correlation for solvents with higher χ and higher P_v (See Figure S10, Supporting Information for the sensor response at different analyte concentration) to cause a faster quenching, except for CP exposed to chloroform. This might be because the systems' thickness and polarity are not accounted for in the calculations. As discussed earlier, the quenching kinetics appear to be multi-staged and complex. In fact, multiple interfering mechanisms, including solvent accumulation at the barriers, diffusion acceleration at the layer interfaces, and molecular relaxation could be at play, as reported for similar systems in the literature.[19,25]

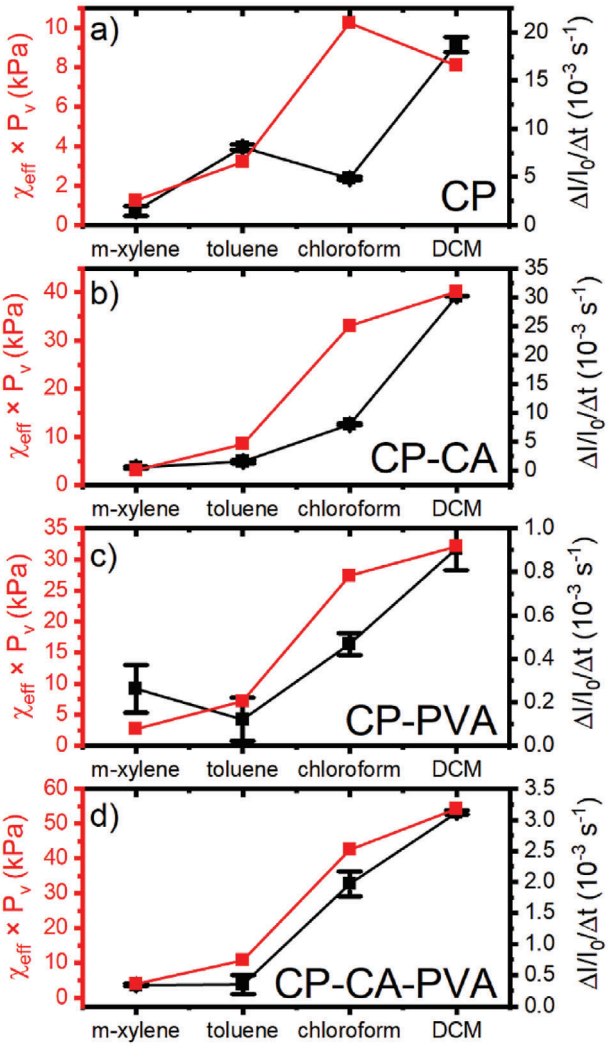

Figure 5. Quenching rate (black squares) and the product of the χ_{eff} and P_v for the a) CP, b) CP-CA, c) CP-PVA, and d) CP-CA-PVA films on exposure to different analytes.

3. Conclusion

In summary, we demonstrate that a random copolymer of polystyrene and the fluorescent AIEgen JCBF is a promising disposable solid-state vapor sensor. We probed its fluorescence intensity as a thin film and the influence of exposure to different volatile organic compounds on it. Most importantly, we demonstrate that simple capping layers of different polymers can be a versatile and simple tool for controlling the specificity of the response of the thin-film sensor without changing the used polymers. While exploratory, the results are promising for both

Figure 4. Fluorescence intensity quenching as a function of exposure time for: a) CP film, b) CP capped with CA, c) CP capped with PVA, and d) CP capped with both CA and PVA on exposure to *m*-xylene (red), toluene (blue), chloroform (green) and DCM (orange). e) Quenching extent for fluorescent films after exposure to different analytes after 20 min.

sensing applications as well as investigations of diffusion kinetics in polymer matrices.

4. Experimental Section

Synthesis of P(STY-co-JCBF): JCBF and P(STY -co-JCBF) were synthesized and characterized according to the literature.[19] For the synthesis of the random copolymer, a solution of JCBF (0.025 mmol), styrene (4.800 mmol) and azobisisobutyronitrile (AIBN, 0.037 mmol) in 5 mL of anhydrous toluene was introduced into a dry reaction tube and the polymerization was let to proceed at 60 °C for one week. The polymer was then recovered by precipitation in methanol with a yield of 40% and a JCBF content of 0.34 mol%. The number average molecular weight of P(STY -co-JCBF) was Mn = 11 000 g mol^{-1} with a polydispersity of Mw/Mn = 1.6, a glass transition temperature Tg = 102 °C, and degradation temperature of Td = 420 °C.

Thin Film Fabrication: The CP P(STY -co-JCBF) was dissolved in chloroform to give solutions of 5, 8, 10, and 20 mg mL^{-1}. The solution was stirred for 24 h before casting. The solutions were then spun at 20 revolutions per second (rps) for 20 s onto square glass substrates (1 inch side) or round fused silica substrates (1.5 cm diameter). Solutions of cellulose acetate (CA, Sigma Aldrich, Mw 46 000) and poly(vinyl alcohol) (PVA, Sigma Aldrich, Mw 40 000) at a concentration of 30 mg mL^{-1} in diacetone–alcohol and water/ethanol mixtures (75:20), respectively, were cast by dynamic spin coating at 175 rpm. In this case, the solution was also stirred for 24 h before deposition. All films were stored in Petri dishes and dried in the dark under room conditions for at least 24 h before use. The films cast from the solution CP with a concentration of 8 mg mL^{-1} were used to prepare the sensors. They were either used as is or coated with a layer of CA, PVA, or both polymers. CA was treated with 30 s air plasma (Gambetti, Colibri) prior to PVA deposition to improve coverage and homogeneity of the subsequently cast PVA film. Since the thickness of the polymer film has an influence on the molecular diffusion coefficient in polymer films[25] and thus on the response kinetics, all samples were prepared under identical conditions to avoid being influenced by this parameter.

Absorbance Measurements: Absorbance measurements were performed using UV-1800 Spectrophotometer (Shimadzu, Kyoto, Japan).

Reflectance Measurements: Reflectance was recorded through a customized optical fiber-based setup consisting of deuterium and tungsten-halogen sources (Micropak, DH2000BAL, spectral range 230–2500 nm) employing reflectance from a UV-enhanced aluminum mirror (Thorlabs, PF10-03-F01) as a reference. The light was transmitted to and from the sample through an optical fiber (Avantes, FCR-7UVIR200-2-ME) and was detected through an AvaSpec-ULS4096CL-EVO spectrometer (CMOS, spectral range 200–1100 nm, resolution 1.4 nm).

Analytes: The tested analytes were chloroform (anhydrous, >99%, Sigma–Aldrich), dichloromethane (DCM, anhydrous, ethanol stabilized, SupraSolv, Supelco), toluene (ACS reagent, >99.5% Sigma–Aldrich), *m*-xylene (ReagentPlus, 99%, Sigma–Aldrich).

Fluorescence Intensity Measurements: Films were cut into ≈10 × 7 mm^2 rectangles for fluorescence measurements during vapor exposure. These were performed in a custom-built setup schematized in Figure S1 (Supporting Information). The samples were placed inside a fused silica (Hellma QS macrocells) cuvette at 45° to avoid collecting edge-guided fluorescence signals as well as reflected laser beams. The optical fibers-based setup allowed the facile collection of the fluorescence signal during exposure to analyte vapors. Fluorescence variations were collected upon CW excitation with an Oxxius 405 nm continuous wavelength laser focused on a 1 mm^2 spot. The fluorescence signal was collected using the same spectrometer used for reflectance measurements. Long-pass optical filters (RazorEdge LP 442 RE and EdgeBasic LP 205 R, Semrock) were used for the collected fluorescence to eliminate the excitation laser signal. Excitation and collection were performed at 90°. Vapor exposure was achieved by adding ≈0.5 mL of the desired analyte to a glass pouch and allowing the closed pouch to be saturated with the vapor at room temperature (Figure S1, Supporting Information). Afterward, the bulb was fitted to the cuvette, and the fluorescence was recorded each second for 20 min. Fluorescence of the solutions was measured using the same excitation source, fibers and spectrometer while changing the holder to allow for appropriate excitation/collection geometry.

Thickness Measurements: Film thicknesses were determined through Atomic Force Microscope (AFM) measurements through the scratch method. The films were first scratched, and the profile was measured to determine the height of the polymer film. Measurements were performed in tapping mode using Nanosurf CoreAFM microscope. Analyses of the scans were performed using the open-source software Gwyddion.[30]

Statistical Analysis: Measurements of steady-state absorption and PL were normalized to maximum spectral intensity. Quenching measurements were normalized by the maximum spectral intensity at zero exposure time. Quenching dynamics were determined after normalization as the emission intensity at 480 nm. Quenching values were derived from the quenching dynamics at a given time. No outliers were excluded. the χ-values were calculated according to Equation (2). All data analyses and fits were performed using OriginLab software, with errors represented by x ± standard deviation.

Supporting Information

Supporting Information is available from the Wiley Online Library or from the author.

Acknowledgements

P.L. acknowledges the Departments of Chemistry and Industrial Chemistry for the financial support. A.P. acknowledges MIUR through the PRIN project 20179BJNA2 for financial support. Pierpaolo Minei and Giuseppe Iasilli are kindly acknowledged for their support in the fluorescent copolymer preparation.

Conflict of Interest

The authors declare no conflict of interest.

Author Contributions

H.M. performed the experiments, analyzed the data, and drafted the manuscript. L.M., M.M., and P.L. performed absorbance and some quenching experiment. P.L., M.C., A.P., and D.C. provided funding, materials, supervision and edited the manuscript.

Data Availability Statement

The data that support the findings of this study are available from the corresponding author upon reasonable request.

Keywords

aggregation-induced emission, fluorescent sensors, molecular diffusion, polymer thin films, volatile organic compounds

Received: July 20, 2023
Revised: August 18, 2023
Published online:

[1] H. Guo, S. C. Lee, L. Y. Chan, W. M. Li, *Environ. Res.* **2004**, *94*, 57.

[2] P. Wang, W. Zhao, *Atmos. Res.* **2008**, *89*, 289.
[3] a) J. A. Koziel, J. Pawliszyn, *J. Air Waste Manage. Assoc.* **2001**, *51*, 173; b) K. Demeestere, J. Dewulf, B. De Witte, H. Van Langenhove, *J. Chromatogr. A* **2007**, *1153*, 130; c) N. Ochiai, S. Daishima, D. B. Cardin, *J Environ. Monit.* **2003**, *5*, 997.
[4] A. P. Demchenko, in *Introduction to fluorescence sensing*, Springer, New York **2008**.
[5] T. Ueno, T. Nagano, *Nat. Methods* **2011**, *8*, 642.
[6] a) F. M. Winnik, *Chem. Rev.* **1993**, *93*, 587; b) S. A. Jenekhe, J. A. Osaheni, *Science* **1994**, *265*, 765.
[7] A. P. Green, A. R. Buckley, *Phys. Chem. Chem. Phys.* **2015**, *17*, 1435.
[8] J. Luo, Z. Xie, J. W. Y. Lam, L. Cheng, H. Chen, C. Qiu, H. S. Kwok, X. Zhan, Y. Liu, D. Zhu, B. Z. Tang, *Chem. Commun.* **2001**, 1740.
[9] X. Du, J. Qi, Z. Zhang, D. Ma, Z. Y. Wang, *Chem. Mater.* **2012**, *24*, 2178.
[10] a) A. Pucci, *Sensors* **2019**, *19*, 4969; b) A. Pucci, in *Handbook of Aggregation-Induced Emission: Emerging applications*, Vol. *3*, Wiley, Hoboken, NJ, USA **2022**.
[11] J. Mei, Y. Hong, J. W. Y. Lam, A. Qin, Y. Tang, B. Z. Tang, *Adv. Mater.* **2014**, *26*, 5429.
[12] Z. Zhao, H. Zhang, J. W. Y. Lam, B. Z. Tang, *Angew. Chem., Int. Ed.* **2020**, *59*, 9888.
[13] S.-C. Lee, J. Heo, H. C. Woo, J.-A. Lee, Y. H. Seo, C.-L. Lee, S. Kim, O.-P. Kwon, *Chemistry* **2018**, *24*, 13706.
[14] a) Y. Ding, W. Li, F. Wang, H. Li, S. Yang, L. Wang, Z. Wang, M. Tebyetekerwa, B. Z. Tang, *Mater. Adv.* **2020**, *1*, 574; b) I. A. Campbell, G. A. Turnbull, *Phys. Chem. Chem. Phys.* **2021**, *23*, 10791.
[15] M. Ahmad, I. Platonova, A. Battisti, P. Minei, G. Brancato, A. Pucci, *J. Polym. Sci., Part B: Polym. Phys.* **2017**, *55*, 1171.
[16] T. Förster, G. Hoffmann, *Z. Phys. Chem.* **1971**, *75*, 63.
[17] M. A. Haidekker, E. A. Theodorakis, *J. Biol. Eng.* **2010**, *4*, 11.
[18] J. Sutharsan, D. Lichlyter, N. E. Wright, M. Dakanali, M. A. Haidekker, E. A. Theodorakis, *Tetrahedron* **2010**, *66*, 2582.
[19] M. Borelli, G. Iasilli, P. Minei, A. Pucci, *Molecules* **2017**, *22*, 1306.
[20] J. Lee, H. T. Chang, H. An, S. Ahn, J. Shim, J.-M. Kim, *Nat. Commun.* **2013**, *4*, 2461.
[21] J. R. Askim, M. Mahmoudi, K. S. Suslick, *Chem. Soc. Rev.* **2013**, *42*, 8649.
[22] A. M. Ullman, C. G. Jones, F. P. Doty, V. Stavila, A. A. Talin, M. D. Allendorf, *ACS Appl. Mater. Interfaces* **2018**, *10*, 24201.
[23] a) H. Megahd, C. Oldani, S. Radice, A. Lanfranchi, M. Patrini, P. Lova, D. Comoretto, *Adv. Opt. Mater.* **2021**, *9*, 2170017; b) P. Lova, G. Manfredi, C. Bastianini, C. Mennucci, F. Buatier de Mongeot, A. Servida, D. Comoretto, *ACS Appl. Mater. Interfaces* **2019**, *11*, 16872; c) P. Lova, H. Megahd, D. Comoretto, *ACS Appl. Polym. Mater.* **2020**, *2*, 563.
[24] X. Jiang, Y. Hao, H. Wang, J. Tu, G. Liu, *Macromol. Res.* **2022**, *30*, 271.
[25] H. Megahd, P. Lova, D. Comoretto, *Adv. Funct. Mater.* **2021**, *31*, 2009626.
[26] C. M. Hansen, in *Hansen solubility parameters: A user's handbook*, CRC Press, Boca Raton, FL **2002**.
[27] W. M. Haynes, D. R. Lide, T. J. Bruno, in *CRC Handbook of Chemistry and Physics*, CRC Press, Boca Raton, FL **2007**.
[28] A. E. Chalykh, I. I. Bardyshev, T. F. Petrova, *Polymers* **2021**, *13*, 2644.
[29] J. Crank, in *The Mathematics of Diffusion*, Clarendon Press, Oxford **1975**.
[30] D. Nečas, P. Klapetek, *Open Phys.* **2012**, *10*, 181.